Postprint of: Majewski A., Chojnacki J., Przychodzeń W., Unexpected Z/E isomerism of N-methyl-O-phosphothioyl benzohydroxamic acids, their oxyphilic reactivity and inertness to amines, STRUCTURAL CHEMISTRY, Vol. 32 (2021), pp. 1077-1091, DOI: 10.1007/s11224-020-01719-1

Query Details

1. **Please check if the section headings are assigned to appropriate levels and amend as deemed necessary.**

   Please, insert an extra line after "O -Phosphothioyl benzohydroxamic acids 3a-3e"

2. **Please check if the tables are presented correctly.**

   The tables are presented correctly.

Original Research

Unexpected Z/E isomerism of *N*-methyl-*O*-phosphothioyl benzohydroxamic acids, their oxyphilic reactivity and inertness to amines

Arkadiusz Majewski, [1]

Jarosław Chojnacki, [2]

Witold Przychodzeń, [2]✉

Email witold.przychodzen@pg.edu.pl

[1] CSL Behring, CSL Behring Lengnau, AG, Industriestrasse 11, 2543 Lengnau, BE, Switzerland

2 Department of Inorganic Chemistry, Gdansk University of Technology, Narutowicza 11/12, 80233 Gdansk, Poland

Received: 12 November 2020 / Accepted: 25 December 2020

Abstract

Thiophosphinoylation of *N*-methyl p-substituted benzohydroxamic acids using disulfanes (method A) or diphenylphosphinothioyl chloride (method B) provides only one conformer of the respective *O*-phosphothioyl derivative (X-ray and NMR analysis). Undergoing the *P*-transamidoxylation reaction is an evidence of the reversibility of thiophosphinoylation. Only those products containing strong EWG substituents in the aroyl residue or bulky substituents at the phosphorus atom possess *E* conformation. DFT calculations confirmed the energetic domination of each isomer. The *Z*-isomers are distorted amides having both high degree of nitrogen pyramidalization (38–55°) and amide twist (12–30°). In solution they exist in a defined conformation that is evidenced by the presence of a sharp signal of *N*-methyl protons at low temperature. They do not isomerize in solutions. Some of them slowly undergo the N-O bond scission above 100 °C. Both isomers are not as sensitive to neutral hydrolysis as twisted amides can be and are inert toward amines. The rate of alkaline hydrolysis can be correlated with pKa of hydroxamic acid. Because of their outstanding oxyphilicity, these compounds can be defined as nerve agent surrogates and safer alternatives of phosphorus fluorides for serine-active enzyme inhibition studies.

Keywords

Hydroxamic acids
Thiophosphinoylation
Z-E isomerism
Crystal structure
NMR analysis
Hydrolysis

Supplementary Information

The online version contains supplementary material available at https://doi.org/10.1007/s11224-020-01719-1.

Introduction

Organophosphorus nerve agents are still a threat to the international community. Their structure, treatment [1] and, in particular, the hydrolysis [2, 3] are the subject of interest of research centres, in particular, to their potential usage as poisons.

Hydroxamic acids (HAA) are natural compounds with a variety of biological activity such as anti-inflammatory, anti-virus, antitumor, and anti-oxidant activities [4, 5]. Four of them are marketed anticancer (varinostat, belinostat, panobinostat) and anti-infection (Lithostat) drugs [6]. Among hydroxylamine derivatives, they were involved occasionally for organophosphorus biocide (OPB) detoxification studies. The corresponding *O*-phosphorylated HAA are believed to be key intermediates in chemical transformations involving OPB and HAA. *N*-Unsubstituted HAA as powerful α-nucleophiles promote hydrolytic cleavage of OPB. Initially formed *O*-phosphoyl HAA are hydrolysed giving phosphate as a final product after Lossen rearrangement [7]. Electron donating-substituted benzohydroxamic acids are even more effective; e.g. sodium 4-metoxybenzohydroxamate accelerates hydrolysis of sarin (*O*-isopropyl methylphosphonofluoridate) by a factor 500 relative to unsubstituted one [8].

Unlike *N*-unsubstituted HAA, *N*-alkyl HAA do not undergo Lossen degradation and can regenerate. Additionally, *N*-alkyl HAA were considered far more efficient detoxicants against electrophilic OPB than unsubstituted ones in biphasic systems [9]. For the reaction between 4-nitrophenyl diphenylphosphinate and sodium 4-methoxy 4-methylbenzohydroxamate, up to 300 times acceleration was found as compared to sodium 4-chlorophenolate [10]. One can speculate that the respective *O*-phosphoylated hydroxamic acids are generated, although knowledge about their structure and reactivity is still under open debate. They can be classified as dynamically expanding group of nerve agent surrogates, safe alternatives for novel acetylcholinesterase (AChE) reactivators and biochemical, toxicological and analytical tools [11].

N-Alkyl HAA are less frequently studied than unsubstituted as potential therapeutics as antiviral [12] and anticancer agents [13, 14], albeit they are mainly found in nature and are non-mutagenic.

N-Alkyl-*O*-phosphothioyl HAA are quite new and relatively unexplored class of compounds with interesting structure and unpredictable reactivity. They are also formed as intermediates in the reaction of HAA and Lawesson reagent [15] as well as stable products of their thiophosphinoylation using bisphosphothioyl disulfanes [16]. On the other hand, protective phosphothioyl groups have been used occasionally for protection of amine, hydroxyl and thiol functions in organic synthesis [17], among them the diphenylphosphinothioyl [18] and the diisopropoxyphosphinothioyl [19] for selenols protection.

N-Methyl-*O*-phosphothioyl benzohydroxamic acids **3** are formally mixed anhydrides of benzohydroxamic BHAA (pKa 7.9–8.6 [20]) and phosphothioic acids (pKa 1.5–3.9 [21]). Their behaviour toward nucleophilic agents is difficult to predict, because nucleophiles can split the P-O as well as the C(=O)-O or the N-O bonds. Although nucleophilic substitution on the nitrogen atom of hydroxamic acid derivatives is rare and is limited only to so-called anomeric amides [22, 23], such transformation cannot be excluded, especially when the respective nitrogen atom is highly sp^3 hybridized (as in twisted amides). According to HSAB theory, the direction of the nucleophilic attack depends on the hardness of a nucleophile; i.e. hydroxide, as a hard base, would prefer a hard phosphorus atom.

We have previously proved that the reaction of hard sodium 4-chloro-*N*-methyl benzohydroxamate **1b-Na** with *bis*phosphothioyldisulfanes **2**, affords the abovementioned derivatives **3** in high yield [16]. We proved that thiophosphinoylation of hydroxamates with **2** has limitations for other *N*-alkyl BHAA. We found that both branching of the *N*-alkyl moiety and electron-donating character of the aroyl group causes a change of the ionic into radical pathway of the reaction. It is apparently connected with the extra stabilization of the respective *N*-*tert*butylaminoxyl radicals as well with a greater electron density and a lower oxidation potential of electron-rich hydroxamates. Therefore, we proved that the reaction occurs exclusively by a pure radical mechanism for *N*-*tert*butyl benzohydroxamate and its mixed radical-ionic nature significantly reduces the yield of **3** in the case of *N*-isopropyl benzohydroxamates and *N*-methyl-4-methoxy benzohydroxamate **1a-Na**.

Phosphoryl chlorides are most commonly used in the synthesis of *O*-phosphotoylated HAA **3**, the availability of which, stability and, not least, toxicity are the basic limitations of this method [24].

It seems obvious that due to the formation of strong intermolecular H-bonds, BHAA in the crystalline state must exist in the form of *E* isomers. However, there are exceptions such as *N*-phenyl benzohydroxamic acid, whose crystals obtained from acetone consist of molecules with a *Z*-conformation [25]. Among *N*-isopropyl BHAA, we found that both p-methoxy substituted one and 3,5-dinitro-substituted exist in the form of *E* isomers in the crystalline state, while in solution the first of them takes the *Z*-conformation and for the second both forms have nearly equal populations [26]. Conformation of p-methyl and p-methoxy *N*-methyl BHAA was investigated by Brown, and he found that they adopt *E*-conformation in crystal state and mainly *Z*-conformation in $CDCl_3$ solution [27]. Kalinin [28] studied the conformational behaviour of a series of *N*-methyl BHAA (including p-chloro substituted). He showed that their CD_2Cl_2 solutions in − 70 °C contain 66–73% of *Z* isomer and the Z/E ratio does not depend on the Hammett constant of the substituent.

Experimental

Computational methods

All calculations have been carried out with the *Gaussian 03W* package [29, 30]. The starting coordinates were prepared by extracting the atomic coordinates from the X-ray crystal structures. The geometry of molecules studied has been optimized using the B3LYP/6-311+G(dp) method. Each optimization was followed by IR frequency calculations to test whether the optimal points are true minima or just saddle points. All appeared to be minima. Energy barriers to rotation for **3d** and **3c** were calculated at B3LYP/6-31G(d) level of theory by relaxed scanning of the O2-C2-N1-O1 dihedral.

General

All NMR spectra were recorded on a Varian Unity 500 Plus spectrometer operating at 500 MHz (^{1}H), 202.4 MHz (^{31}P) and 125.7 MHz (^{13}C) in deuterated solvents ($CDCl_3$, CD_2Cl_2, $C_2Cl_2D_2$, CD_3OD, aceton-d_6). ROESY difference spectra for compounds **3a** and **3c** were recorded with 0.3 s mixing time. FT-IR spectra (solid and 20 mM chloroform solutions, resolution of 4 cm^{-1}, in the range of 500–5000 cm^{-1}, 64 independent scans) were recorded on the Nicolet 8700

spectrometer (Thermo Electron Co.) with a single-reflection diamond crystal Golden Gate ATR accessory (Specac). Mass spectra were measured with an AMD-604 double-focusing mass spectrometer (EI method) and a MARINER (ESI-TOF) PerSeptive Biosystems spectrometer (ESI method). TLC analyses were performed on silica gel 60 F254 precoated on aluminium sheets (Merck). THF was distilled from benzophenone ketyl, methanol from magnesium methoxide, DCM from CaH_2 and toluene from sodium under nitrogen. Aroyl chlorides (4-methoxybenzoyl chloride, 4-chlorobenzoyl chloride and 4-nitrobenzoyl chloride), *N*-methylhydroxylamine hydrochloride, chlorodiphenylphosphine, DBU and triethylamine were purchased from Sigma-Aldrich (Poznań, Poland). Disulfanes **2** were obtained as previously described [16].

Diphenylphosphinothioyl chloride **4** and diphenyl 4-nitrophenyl phosphinothioate **8** were prepared according to procedures by Harger [31] and Williams [32], respectively. An authentic sample of *N*-methyl-4-methoxybenzamide **5a** was obtained from 4-methoxybenzoyl chloride. Diphenylphosphinothioic acid amide **7** and *O*-methyl diphenyl phosphinothioate **6** were synthesized from chloride **4** following the procedure described in Ref. [33, 34] and by Kabachnik [35], respectively.

***N*-Hydroxy-*N*-methylbenzamides 1a-1c** were prepared using to a standard procedure [36].

To a stirred solution of methylhydroxylamine hydrochloride (1.4 g, 17 mmol) and triethylamine (4.3 ml, 31 mmol) in 5 ml DCM, a solution of the corresponding aroyl chloride (14 mmol) in anhydrous DCM (5 ml) was added dropwise over 1 h at 0 °C. After the addition was complete, the reaction mixture was allowed to warm to room temperature and stirring was continued overnight. Next, it was concentrated in vacuo and dissolved in ethyl acetate (25 ml). The organic layer was then washed successively with equal volumes (5 ml of each) of water, 0.5 M HCl, water, a 10% $NaHCO_3$ solution, water and brine. The organic layer was dried over $MgSO_4$ and concentrated. The solid residue was recrystallised to give the pure benzohydroxamic acid **1**.

***N*-Hydroxy-4-methoxy-*N*-methylbenzamide 1a** (74%), white crystals, mp 106–108 °C (ethanol, lit. mp [37] 109–112 °C)

4-Chloro-*N*-hydroxy-*N*-methylbenzamide 1b (73%), white crystals, mp 115–117 °C (toluene, lit. mp [21] 118–120 °C)

***N*-Hydroxy-*N*-methyl-4-nitrobenzamide 1c** (57%), light yellow crystals, mp 171–172 °C (ethanol, lit. mp [21] 171–172 °C)

O -Phosphothioyl benzohydroxamic acids 3a-3e

Method A

AQ1

[16]

To a stirred solution of the corresponding *N*-methyl benzohydroxamic acid **1** (0.5 mmol) in THF (7 ml), NaH (0.015 g, 0.62 mmol) was added and the mixture was stirred under argon. When hydrogen evolution was ceased, the mixture was refluxed for 1.5 h and next disulfane **2** (0.25 mmol) was added in one portion at rt. After 1 h, the reaction was concentrated in vacuo and the residue applied to a silica gel column. Elution with $CHCl_3$ gives pure *O*-diphenylphosphinothioyl benzohydroxamic acid **3**.

Method B

To a stirred solution of the corresponding *N*-methyl benzohydroxamic acid **1** (2.5 mmol) in dry dichloromethane (25 ml), DBU (0.373 ml, 2.5 mmol) was added at 5 °C. After 15 min, a solution of diphenylphosphinothioyl chloride **4** (0.63 g, 2.5 mmol) in 10 ml of dichloromethane was added dropwise during 1 h. After 16 h, the solvent was evaporated and the oily residue was chromatographed on silica gel to give pure *O*-diphenylphosphinothioyl benzohydroxamic acid **3**.

N -Methyl- *N* -diphenylphosphinothioyloxy 4-methoxybenzamide 3a

Method A: yield 81%

Method B: yield 70%, mp 134-7 °C (benzene-cyclohexane)

^{1}H NMR: δ = 3.48 (s, 3H, NCH_3), 3.82 (s, 3H, OCH_3), 6.82 (d, *J* = 8.8 Hz, 2H, H3/5), 7.44 (d, *J* = 8.8 Hz, 2H, H2/6), 7.45 (dt, *J* = 7.3 and 3.8 Hz, 4H, H3’/5’), 7.51 (dt, *J* = 7.3 and 1.5 Hz, 2H, H4), 8.03 (dd, *J* = 13.7 and 7.3 Hz, 4H, H2’/6’) ppm. ^{13}C NMR: δ = 43.9 (NCH_3), 55.6 (OCH_3), 113.9 (C3/5), 125.4 (C1), 128.5 (d, *J* = 13.4, C3’/6’), 130.9 (C2/6), 132.3 (d, *J* =

11.7 Hz, C2'/6'), 132.4 (d, *J* = 107 Hz, C1'), 132.7 (d, *J* = 3 Hz, C4'), 162.4 (C4), 173.3 (C=O) ppm. ^{31}P NMR: δ = 95.2 ppm.

IR: 1699 cm^{-1} ($\nu_{C=O}$)

HRMS (ESI): calcd. for $C_{21}H_{20}NO_3PS^{35}Na$ 420.07938; found 420.07863.

MS (EI, 70 eV) m/z (%): 135 (26) $ArCO^+$, 217 (30) Ph_2PS^+

***N*-Methyl-*N*-diphenylphosphinothioyloxy 4-chlorobenzamide 3b**

Method A: yield 89%

Method B: yield 70%, mp 83–85 °C (ethyl acetate – hexane, lit. mp [16] 83–85 °C)

IR: 1705 cm^{-1} ($\nu_{C=O}$).

***N*-Methyl-*N*-diphenylphosphinothioyloxy 4-nitrobenzamide 3c**

Method A: yield 70%

Method B: yield 64%, mp 120–4 °C (benzene-cyclohexane)

^{1}H NMR: δ = 3.45 (s, 3H, NCH_3), 7.41 (dt, *J* = 7.4 and 3.4 Hz, 4H, H3'/5'), 7.52 (dt, *J* = 7.4 and 1.4 Hz, 2H, H4'), 7.63 (d, *J* = 8.8 Hz, H2/6), 7.77 (dd, *J* = 13.7 and 7.3 Hz, 4H, H2'/6'), 8.07 (d, *J* = 8.8, 2H, H3/5); ^{13}C NMR: δ = 40.1 (NCH_3), 123.1 (C2/6), 128.4 (d, *J* = 13.7, C3'/6'), 129.6 (C3/5), 131.4 (d, *J* = 11.4, C2'/6'), 132.0 (d, *J* = 105 Hz, C1'), 132.6 (d, *J* = 3 Hz, C4'), 139.8 (C1), 148.6 (C4), 169.6 (C=O); ^{31}P NMR: δ = 95.4 ppm.

IR: 1641 cm^{-1} ($\nu_{C=O}$)

HRMS (ESI): calcd. for $C_{20}H_{17}N_2O_4PS^{35}Na$ 435.05389; found 435.05495.

MS (EI, 70 eV) m/z (%): 150 (35) $ArCO^+$, 217 (100) Ph_2PS^+.

***N*-Methyl-*N*-[isopropylamino(4-methoxyphenyl)-phosphinothioyloxy] 4-chlorobenzamide 3d**

Method A: yield 91%, mp 143–4 °C (ethyl acetate–hexane, lit mp [16] 143–4 °C)

IR: 1691 cm^{-1} ($\nu_{C=O}$)

(S_P)-*N*-Methyl-*N*-[(–)-menthoxy(4-methoxyphenyl)phosphinothioyloxy] 4-chlorobenzamide 3e

Method A: yield 90% mp 105–107 °C (acetonitrile, lit mp [16] 105–107 °C)

Hydrolysis experiments

Hydrolysis experiments of **3** were conducted in a NMR tube and were monitored using ^{31}P NMR and/or TLC.

Hydrolysis of 3: To a solution of **3** (0.1 mmol) in THF-water (3:1, 0.5 ml) containing one drop of C_6D_6 as a lock solvent DBU (0.030 ml, 0.2 mmol, 2 eq for **3a - 3c** or 0.060 ml or 0.4 mmol, 4 eq for **3d**) was added. For reactions involving **3a – 3c**, the progress of the reaction was monitored by recording ^{31}P NMR spectra at various time intervals, at rt.

Hydrolysis of 4: To a solution of **4** (0.1 mmol) in THF-water (6:1, 0.5 ml) DBU (0.030 ml, 0.2 mmol) was added. After 40 min at rt, TLC analysis showed the absence of **4**.

Hydrolysis of 8: To a solution of **8** (0.1 mmol) in THF-water (3:1, 0.5 ml), DBU (0.030 ml, 0.2 mmol) was added and the reaction is monitored by measuring the absorbance of the p-nitrophenolate anion (at λ_{max} = 400 nm) at various time intervals.

Ammonolysis experiment

3b (40 mg, 0.1 mmol) is dissolved in 2 ml of 10 M ammonia methanolic solution. After 5 h at rt, ^{31}P NMR analysis showed that the reaction mixture contained approximately 93% of *O*-methyl diphenylphosphinothioate and trace amount of diphenylphosphinothioic amide (7%) as the only products.

Aminolysis experiment

To a solution of **3b** (40 mg, 0.1 mmol) in 1 ml of DCM anhydrous benzylamine (13 µl, 1.2 eq) was added and the resulting solution was stirred for 16 h. After this time, TLC and ^{31}P NMR analysis showed the presence of unchanged starting material.

P-transamidoxylation (an exchange experiment)

To a stirred solution of **1a** (0.045 g, 0.375 mmol) in 5 ml of THF, sodium hydride (11 mg, 0.45 mmol, 1.2 eq) was added in one portion at rt. After hydrogen evolution ceased, **3c** (0.103 g, 0.25 mmol, 1 eq) was added in one portion. The progress of the reaction was monitored by TLC (hexane-AcOEt 6:1; 10-times developing; $R_{f(3a)} = 0.37$, $R_{f(3c)} = 0.37$). After 48 h at rt, the mixture was evaporated, dissolved in chloroform and chromatographed on silica to separate from polar hydroxamic acids salts. ^{1}H NMR analysis in $CDCl_3$ revealed that the mixture contains **3a**/**3c** = 54:46.

Results and discussion

O-Phosphothioylhydroxamic acids **3** under the study have been prepared by two methods in which *N*-methyl 4-substituted hydroxamic acids **1a - c** were treated with either *bis*(phosphothioyl)disulfanes **2a** – **2d** (method A) **[**16] or with diphenylphosphinothioyl chloride **4** (method B) (Scheme 1). Thus, derivatives **3a - 3c** were obtained by both methods. **3d** and **3e** had to be synthesized exclusively using *bis*phosphonothioyl disulfanes **2a** and **2b**, because the corresponding chlorides **4a** and **4b** could not be isolated in pure form due to partial decomposition during chromatographic purification on silica gel. Alternatively, both protocols were applied to compare the reaction yields. Method A affords slightly better yields of products **3**, probably because the procedure involves twofold molar excess of hydroxamate **1-Na**. Evidently, *bis*anisylphosphothioyl disulfanes **2** are less reactive than chloridate **4** in reaction with hydroxamate **1**, but we confirmed that thiophosphinoylation reaction rate does not affect the preference of specific isomer formation (see below).

Scheme 1

Synthesis routes of *N*-methyl *O*-phosphothioyl benzohydroxamic acids 3.

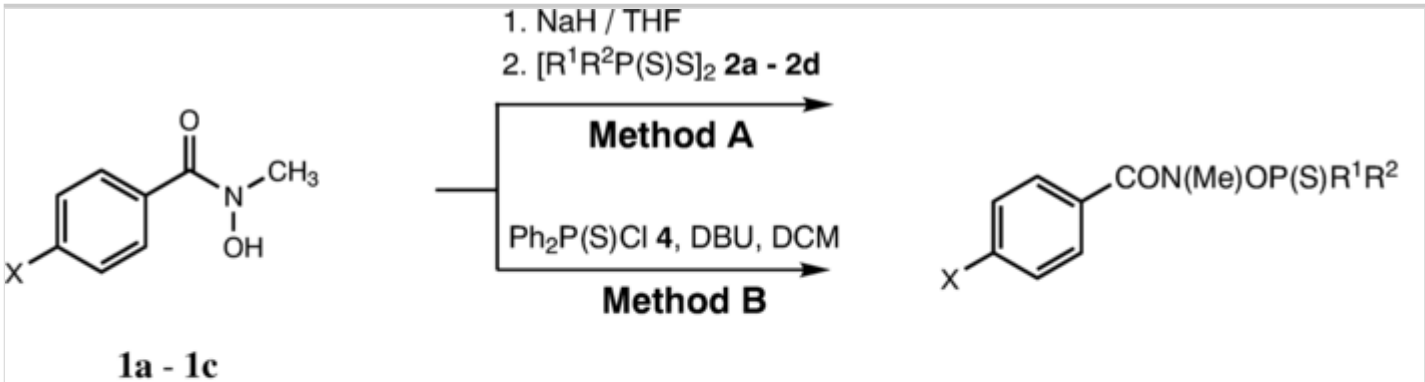

	Method A	Method B
3a X = OCH_3, $R^1 = R^2$ = Ph	81%	70%
3b X = Cl, $R^1 = R^2$ = Ph	89%	70%
3c X = NO_2, $R^1 = R^2$ = Ph	70%	64 %
3d X = Cl, R^1 = 4-$MeOC_6H_4$, R^2 = NHiPr	91%	-
3e X = Cl, R^1 = 4-$MeOC_6H_4$, R^2 = OMenthyl	90%	-

In each case, regardless of the chosen mode of preparation, we isolated only single isomer **3** (Fig. 1), which was confirmed by comparing ^{1}H NMR spectra of both obtained samples (Fig. S7 and S8).

Fig. 1

The structures of specific *Z* and *E* isomers of *N*-methyl *O*-phosphothioyl benzohydroxamic acids 3 along with the atom numbering (ORTEP of (*Z*)-3a as an example) utilized in the discussion

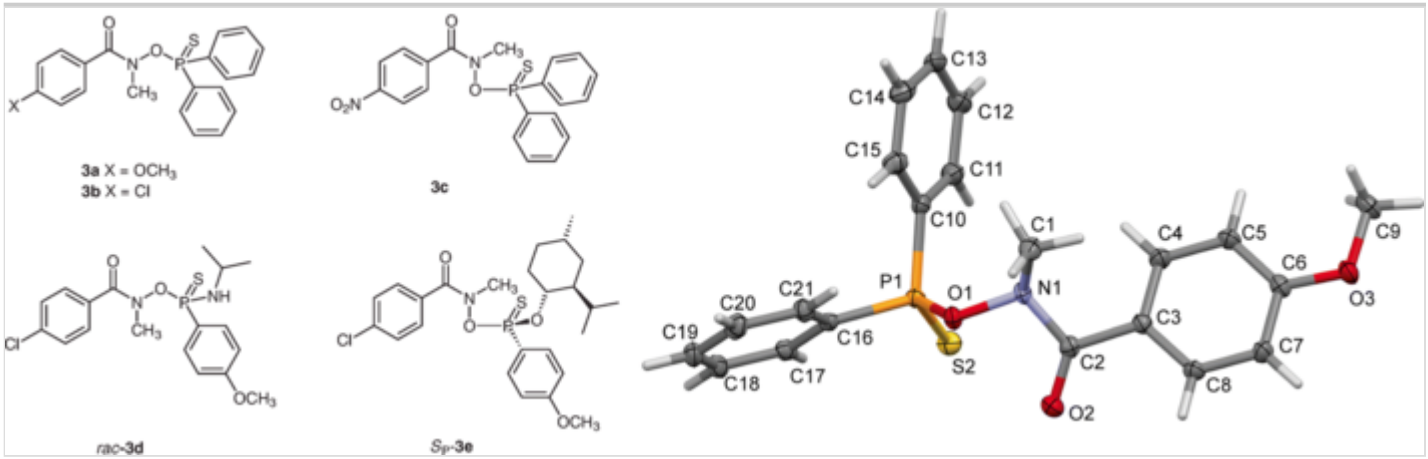

To begin with, we decided to study the Z/E isomerism of the starting BHAA **1a** – **1c**. We confirmed that in crystal state all **1** under the study adopt solely *E*-conformation primarily due to the formation of favourable intermolecular N-OH…O=C bonds (Fig. S44).

It is well-known that in $CDCl_3$ solution *N*-methyl BHAA **1** exist mainly as Z-isomers [28, 29]. The performed ^1H NMR analysis at − 70 °C revealed that starting **1a** and **1c** in chloroform occur as a mixture of both isomers (Z/E 90:10) which was established on the basis of NOE enhancement of H4/8C observed when C1-Me is irradiated (Fig. 2).

Fig. 2

^1H NMR spectra of solutions of **1a** (upper spectrum) and **1c** (lower spectrum) in $CDCl_3$ at − 70 °C and the accompanying the results of NOE experiments showing twice larger enhancement for Z-isomers

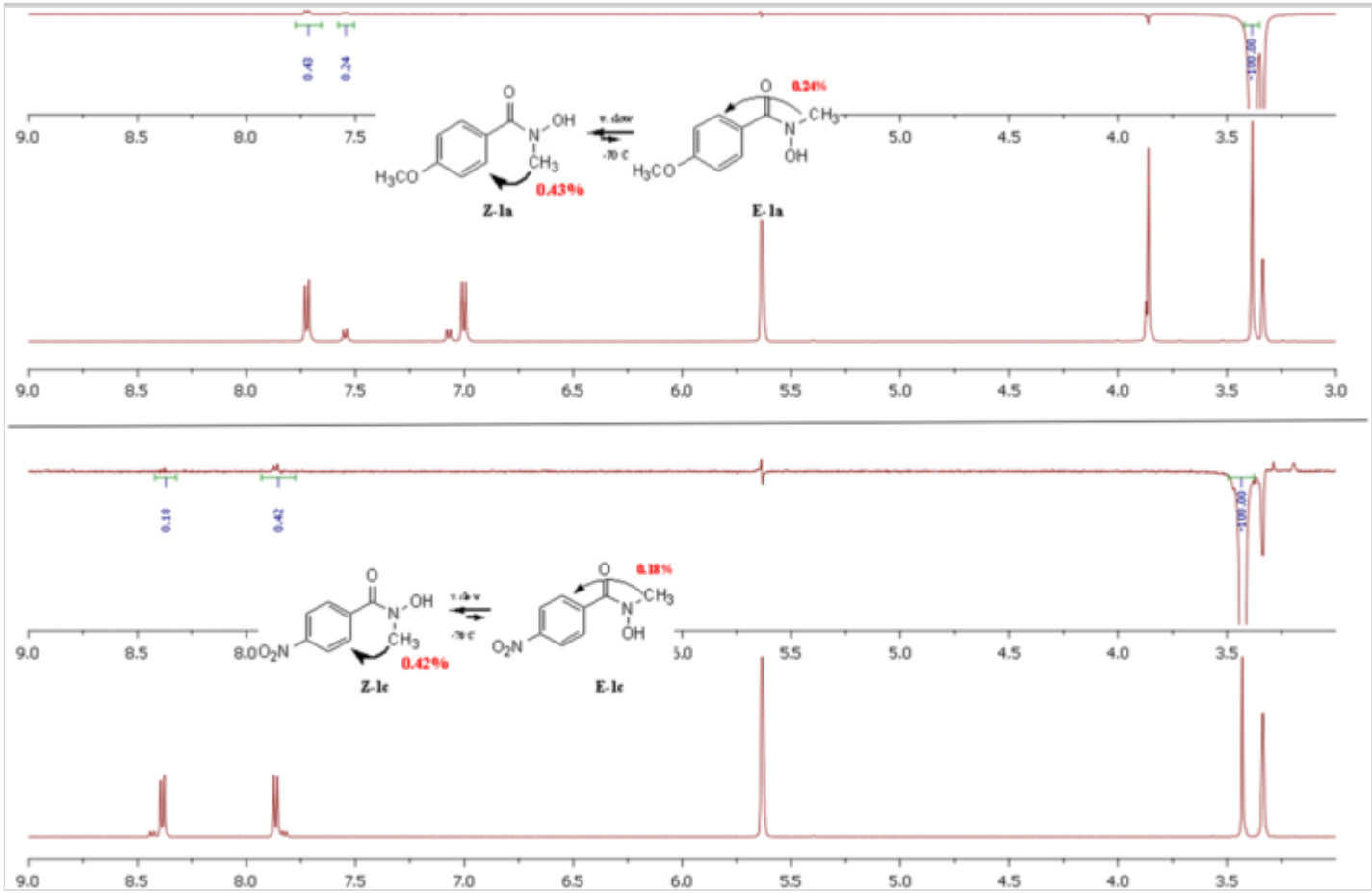

That means that the p-substituent does not influence Z-isomer domination and that the Z/E ratio is not disrupted by changing p-substituent from a strong EDG- (-OMe) to a strong EWG-one (-NO_2). This finding is consistent with Kalinin's finding, but suggests a lower percentage of the Z isomer (66–73%) [29, 30]. It is obvious that when considering the impact of the structure of the starting material **1** on the structure of the product **3**, rather the salt **1-Na** structure should be taken into account. The situation changes upon deprotonation of **1**. ^{1}H NMR spectra analysis confirmed that in deuteriomethanolic solutions sodium salts **1a-Na** and **1c-Na** exist as a mixture of Z and E isomers (Fig. S20 and S21) in 56:44 and 38:62 ratios, respectively, already at room temperature. The methyl signals of **Z-1** and **Z-1-Na** were assigned unambiguously once again based on the NOE experiments. The existence of nearly equally populated mixtures of (*Z*)-**1-Na**

and (*E*)-**1-Na** isomers seems surprising, because the concentration of E isomers should be definitely higher due to the repulsion between lone pairs in Z isomers after removal of their H protons. However, using of methanol as a protic solvent causes the E/Z energy difference decreasing or even inverting (e.g. for sodium *N*-phenyl benzohydroxamate in gas phase and in methanol the calculated $\Delta E_{E\text{-}Z} = -14.05$ and +12.10 kcal/mol, respectively [37]). In our case, the $\Delta E_{E\text{-}Z}$ calculated from equilibrium constant depends on the p-substituent and has a significantly lower value, which is + 0.14 and − 0.29 kcal/mol for **1a-Na** and **1c-Na**, respectively. The presence of double signals of aromatic protons at room temperature indicates a much higher barrier to rotation above the C2-N1 bond in sodium benzohydroxamates **1-N*a*** (i.e. under the actual preparation conditions). Therefore, assuming that salts of **1a** and **1c** exist as nearly equimolar mixture of both isomers, we state that formation of **3** is controlled thermodynamically independent of thiophosphinoylating agent used.

Therefore, it is not clear why derivatives **3** can adopt both stable conformations, which at first glance is not dependent on the nature of substituents in the acyl as well in the thiophosphinoyl residue. Unexpectedly, this preference concerns their conformation in solution, too (see below). We selected one representative of each of the isomers, i.e. **3a** and **3c**, for spectroscopic studies and proved the existence of only one isomer in chloroform solution which conformation is close to that in crystal.

One explanation originates from the consideration of different modes of their preparation. As was mentioned above, deprotonation of **1a-c** is not complete during proceeding the reaction by the use of DBU. In such conditions, both forms (*E* and **Z**) of **1-Na** are thiophosphinoylated and the product distribution should depend on the difference of their concentration assuming that both processes have equal rates. It turned out that the tested reaction of sodium BHAA **1-Na** with bisphosphothioyl disulfanes **2** is irreversible in respect to the formed phosphodithioate, but most importantly, it is reversible with respect to **1-Na** (which was used in excess as a reminder). It was successfully supported by performing an exchange experiment between **3c** and **1a-Na** leading to a mixture of **3a** and **3c** (Scheme 2) in a ratio 54: 46 determined by ^{1}H NMR analysis (see Fig. S22). Thus, the formation of **3** proceeds with a thermodynamic control and favours a more stable isomer. However, the statement of thermodynamic control of the reaction does not explain why only *E*-isomer of **3c** is formed despite the small difference in calculated energy of both isomers (see Table 1). It is possible that the calculations underestimated the real energy differences for **3** not considering the crucial influence of the solvent (see IR spectra analysis below).

Scheme 2

An exchange experiment confirming the reversibility of mixed anhydrides 3 formation

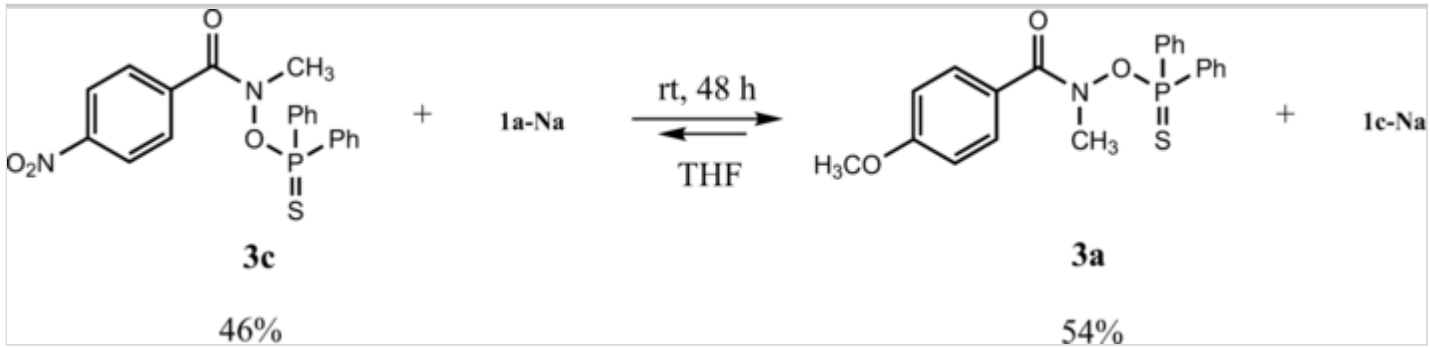

Table 1

Energies from B3LYP/6–31G(dp) calculations (in gas phase) for real 3 (in bold) and hypothetical opposite isomers 3′ (in italics) used for the prediction of the isomer preference at 298 K

	E **(Hartrees)**	***Z*** **(Hartrees)**	$\Delta\Delta G_{Z\text{-}E}$ **(kcal/mol)**	$K_{Z/E}$	**Z/E %**
3a	*−1832.56695115*	**−1832.56928116**	−1.46	11.77	92/8
3b	*−2177.63267720*	**−2177.63414906**	−0.92	4.73	83/17
3c	**−1922.57406458**	*−1922.57336397*	+0.44	0.48	32/68
3d	*−2234.11848523*	**−2234.12245094**	−2.49	67.03	99/1
3e	**−2234.12245094**	*−2234.11848523*	+2.48	0.02	1/99

Performed calculations confirmed that every isolated **3** DFT-optimized crystal structure is more stable than the structure of its opposite isomer (Table 1, Figs. 4 and 5). Analysis of the results from Table 2 shows that except (*E*)-**3c**, which should

exist (or form) next to (*Z*)-**3c** due to the smallest energy difference between them, all other isomers are, or at least should be, homoisomeric.

Table 2

Selected crystallographic data, structural and spectral parameters for 3a – 3e

AQ2

	3a	**3b**	**3c**	**3d**	**3e [Ref 16]**
Bond lengths (Å)					
N1-O1	1.444	1.444	1.411	1.414	1.420
C2-N1	1.410	1.408	1.355	1.369 (1.385)[i]	1.361
C2-O2	1.214	1.210	1.230	1.225 (1.230) [i]	1.229
C3-C2	1.484	1.495	1.501	1.498	1.502
P1-O1	1.642	1.643	1.664	1.655	1.648
P1-S2	1.928	1.929	1.925	1.937 (1.953) [i]	1.917
Torsion angles (°)					
ω_1	30.9	36.1	39.5	33.4 (33.7) [i]	32.5

ω_1= C8C3C2O2; ω_2 = O2C2N1O1; ω_3 = S2P1C10C11; ω_3‘= S2P1C16C17; ω_4 = C3C2N1C1; ω_5 = O2C2N1C1

$\chi_N = 180^o + \omega_2 - \varphi_2$.

$\tau = ½ (\omega_4 + \omega_5)$.

[a]Parameter of optimized hypothetical (*E*)-**3d**

	3a	3b	3c	3d	3e [Ref 16]
ω_2	1.0	2.0	174.1	9.1 (170.5) [i]	− 179.4
ω_5	126.4	126.3	− 0.7	150.8 (25.4) [i]	− 7.4
ω_3/ω_3‘	−4.5/− 21.5	0.4 / 29.5	25.0 / 42.9	− 5.0 (59.1) [i]	− 30.0
C1N1O1P1	123.9	124.4	80.4	100.2	83.3
C2N1O1P1	104.2	104.7	94.8	111.9	104.0
Nitrogen pyramidalization (°) and twist					
χ_N	54.6	51.7	−5.2	38.3	6.8
h parameter	0.40	0.41	0.04	0.26 (15.8) [i]	0.05
τ	28.9	28.1	4.1	12.3	3.3
$\Sigma(\tau + \chi_N)$	83.5	79.8	6.3	50.6	10.3
NMR chemical shifts (ppm), vibration frequencies (cm^{-1})					
$\delta_{N\text{-}C\boldsymbol{H}3}/\delta_{N\text{-}\boldsymbol{C}H3}$	3.48/43.9	3.46/42.2	3.45/40.1	3.49/45.0	3.50/40.9
$\delta_{H17/21}/\delta_{C17/21}$	8.03/132.3	7.90/30.3	7.77/131.4	7.91/133.4	7.67/133.8
$\delta_{\boldsymbol{C}=O}$	173.3	171.7	169.6	171.2	170.9

ω_1= C8C3C2O2; ω_2 = O2C2N1O1; ω_3 = S2P1C10C11; ω_3‘= S2P1C16C17; ω_4 = C3C2N1C1; ω_5 = O2C2N1C1

$\chi_N = 180^o + \omega_2 - \varphi_2$.

τ = ½ ($\omega_4 + \omega_5$).

[a]Parameter of optimized hypothetical (*E*)-**3d**

	3a	3b	3c	3d	3e [Ref 16]
δ_P	95.2	94.2	95.4	88.2	93.8
$\nu_{C=O\ solid/solution}$	1700/1690	1710/1660	1640/1660	nm	nm
ω_1= C8C3C2O2; ω_2 = O2C2N1O1; ω_3 = S2P1C10C11; ω_3'= S2P1C16C17; ω_4 = C3C2N1C1; ω_5 = O2C2N1C1					
$\chi_N = 180^o + \omega_2 - \varphi_2$.					
τ = ½ ($\omega_4 + \omega_5$).					
[a]Parameter of optimized hypothetical (*E*)-**3d**					

Another issue to be resolved was the estimation of the rotation barrier around the C2-N1 bond, which is responsible for the mutual *Z*/*E* transformation. The value of barrier to rotation above the amide bond calculated for nitrogen-pyramidal (*Z*)-**3d** in a gas phase of 13.35 kcal/mol is close to that for parent N-methylbenzohydroxamic acid (13 kcal/mol) but far less from that for typical planar amides (~ 20 kcal/mol).

The predicted value of the rotation barrier for (*E*)-**3c** should be greater than the value calculated for (*Z*)-**3d** due to a substantially double bond character in its C2-N1 bond.

As it turns out, however, the calculated height of the rotation barriers could not be verified experimentally because the presence of opposite isomers was not found in the solution (see below).

That is one of the reasons why the main goal of the presented work has become to indicate and describe the characteristic structural features that determinate the preferences of each of the isomers **3**.

Crystal structure

First of all, we thought that a specific isomer predominance may concern its extra stabilization through specific intramolecular interactions which facilitate the packing of molecules. Thus, no stacking interaction is found in (*E*)-**3c** and

(*Z*)-**3d**; however, it can have some influence on packing in (*Z*)-**3a** and (*Z*)-**3b** (for details see Table S2).

However, it should be mentioned that (*Z*)-**3d** molecules can gain additional stabilization energy via forming of two strong intermolecular H-bonds of the N-H…O-C type (H2 - O2, 2.13 A), giving rise to a 14-membered cyclic dimer, which compensates for the lack of π-stackings (Fig. 3). On the other hand, the hypothetical (*E*)-**3d'** molecules can also form intermolecular hydrogen bonds, although we cannot confirm this fact owning to its unknown crystal structure.

Fig. 3

Structure of (*Z*)-**3d** isomers: cyclic dimer from crystal structure with two intermolecular hydrogen bonds between NH…O=C groups (left) and X-Ray (ellipsoids) structure superimposed on the DFT-optimized (sticks) structure of (Z)-**3d** based on the best benzohydroxamate fragment (right)

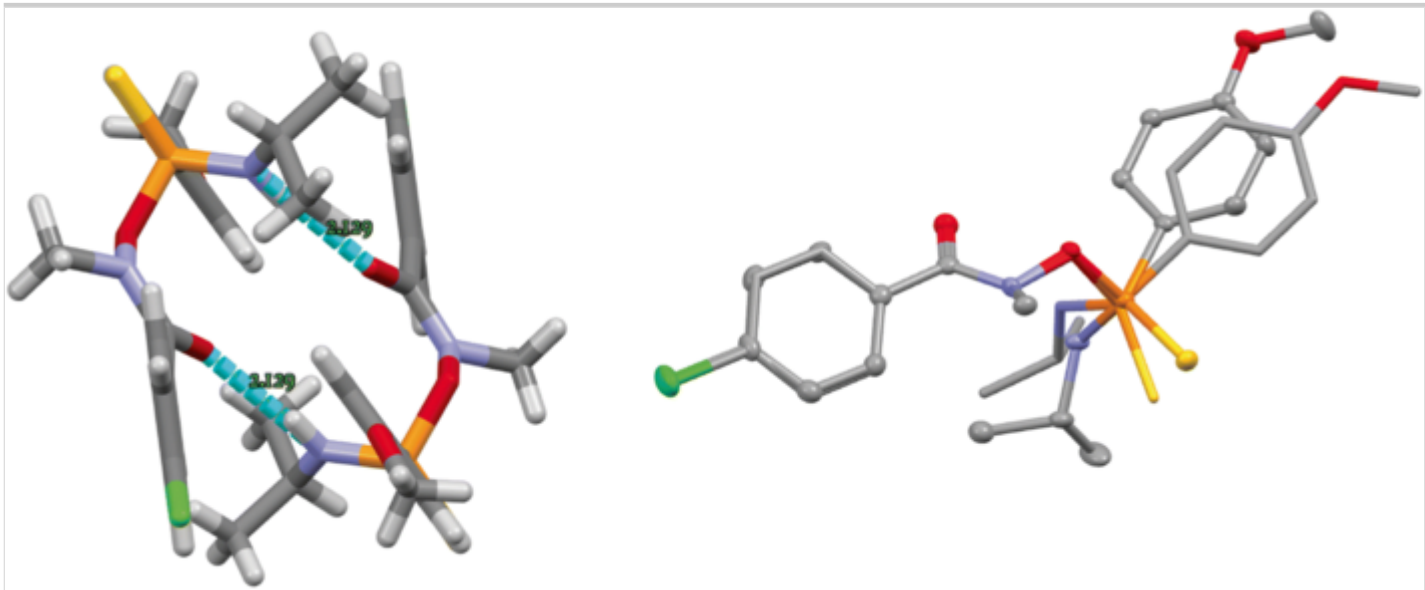

All relevant structural parameters of solid **3** are compared in Table 2.

For *Z*-isomers of **3**, a degree of pyramidalization of the nitrogen atom is remarkable (38–55°). On the other hand, *E*-**3** isomers are only slightly deviated (5° - 7°, 15.8° for calculated E-**3d**). An incomplete conjugation between the carbonyl and the nitrogen lone pair in pyramidalized Z-3 should be manifested in the C-N bond elongation. Indeed, the observed C-N bond in **3a** is 0.055 A (4%) longer than that in **3c** and the respective shortening of the C=O bond is 0.016 A (1.3%). It should be taken into consideration that such effect may be caused by *para*-substituent in aroyl residue. Therefore, it seemed much more reliable to compare the respective structural parameters for *Z*-**3d** and *E*-**3e**, which contain the same p-chlorobenzoyl residue. Thus, it is surprising that the C=O and the C-N bond lengths in **3d** do not differ from those found for **3e** (0.3% and 0.6%, respectively) despite the significant difference in their nitrogen pyramidalization (38.3° and 6.8°, respectively). The twist angle between carbonyl and aryl planes (ω_1) for each aroyl group lies between 30 and 39° and its value does not depend on electronic nature of *para*-substituent and/or substituents at the phosphorus atom, and/or Z/E isomerism. Evidently, regardless of whether the coupling between the aroyl ring electrons and the carbonyl group is partial or complete, the substituents on the phosphorus atom of the thiophosphinoyl residue also have an influence on the hybridization of the nitrogen atom N1 (especially in the case of Z-**3d** and E-**3e**). The consequence of the differences in the carbonyl electron density for **3d** and **3e** is the observed paramagnetic shift (+0.13 ppm) of the H4/8 protons in (*Z*)-**3d**.

The next structural fragment that should be carefully analysed is the surrounding of the N-O bond.

All **3** display favourable arrangement of N-O bond; i.e. both nitrogen pair and the O-P bond are in perfect (for *E*-**3**) and nearly perfect (for *Z*-**3**) eclipsed conformation. It should be added, however, that some HAA derivatives with the bulky O-*tert*butyl substituent can adopt unfavourable staggered conformation and are still stable [33, 34].

Recently, we have noticed that a characteristic feature of the structure of P-anisyl containing solid *bis*phosphothioyl disulfanes **2** is a full conjugation between the P=S and the aryl ring manifested by their planes coplanarity [38, 39]. It should be stressed that the P=S and the phenyl/anisyl group are not coplanar in crystals of *E*-isomers of **3c** and **3e**. The resultant lack of coplanarity expressed by the twist angle (ω_3 and ω_3‘) of 25°–30° causes the P=S bond shortening (Table 1). On the other side, for all Z-isomers of **3**, one P-phenyl ring is always nearly coplanar (ω_3‘ = 0.4–5.0°). Consequently, molecules of *Z*-isomers (**3a**, **3b** and **3d**) lose their resonance stabilization at one side (the amide unit distortion), but can earn it in another place (the arylphosphothioyl residue). On the other hand, *E*-isomers of **3c** and **3e** possess perfectly planar

amide unit at the expense of the arylphosphothioyl distortion. It should be added that the same trend has been found for optimized structure of theoretical *E*-**3d'** isomer which has a planar amide unit and a non-planar arylphosphothioyl residue.

This phenomenon takes places in solution too. It can be proved by ^{1}H NMR spectra where *ortho*-protons (H11/15 and H17/21) of *Z*-**3** isomers are deshielded as compared to the respective protons in (*E*)-**3** isomers ($\Delta\delta_{3a\text{-}3c}$ = 0.26 ppm).

In the solid state, (*Z*)-**3a** possess a higher C=O stretching frequency (1700 cm^{-1}) as compared to (*E*)-**3c** (1640 cm^{-1}) and regular amides (1680 cm^{-1}) (Fig. S23 and S24). It is evidently connected with its nitrogen pyramidalization, because the amide resonance reduces the substituent effect on the carbonyl stretching vibration.

Structure in solution

The structure of **3a** and **3c** in solution was elucidated by the use of NMR and IR analysis.

It has been found that their ^{1}H NMR spectra recorded over a broad range of temperatures (− 50 to + 100 °C) contain single and sharp proton signals of the *N*-methyl groups (Fig. S26 – S28). It can be a strong direct proof for the presence of one isomer in solution. At − 50 °C only multiplets of both kind of aromatic protons in **3c** starts to coalesce which is evidently due to a restricted rotation above the Ar-C(=O) and Ph-P(=S) bonds. It is surprising that broadening of *ortho* protons (H10/17 and H17/21) signal in the PhP=S residue is connected with the respective broadening of *meta*-protons (H5/7) signal in 4-nitrobenzoyl residue. This relationship can be explained by spatial proximity of both protons, found in *E*-**3c** crystal structure, that can be increased by a free rotation above the N-O bond. Further lowering the temperature to − 90 °C leads to the broadening of all aromatic proton signals in *E*-**3c**. Changing the solvent (from CD_2Cl_2 to acetone-d_6) does not affect the observed tendency besides a decrease of the coalescent temperature for H4/8 protons (below − 50 °C) and slight differences in chemical shifts of aromatic all protons.

Therefore, due to complex dynamics of **3** molecules (broadening of signals of the aroyl and the P-phenyl rings), the ROESY experiments for **3a** and **3c** had to be done at room temperature.

Initial experiments performed on starting hydroxamic acids (**1a**, **1c**) and their sodium salts (**1a-Na**, **1c-Na**) allowed isomer identification using the Nuclear Overhauser Effect (NOE) experiments (see above and Fig. 3, S20, S21). Unexpectedly, it

turned out that the enhancing effect also occurs in *E*-isomers, but fortunately it is over two times weaker (0.42% and 0.22% for **1a** and **1c**; 0.99% and 0.47% for **1a-Na** and **1c-Na**).

It should be noted that because the lack of intramolecular hydrogen bonds, the stiffness of the hydroxyamide unit in *Z*-**3** is lower compared to the original *Z*-**1**. Additionally, in the solution we are not dealing with a pure *Z*-conformation but probably with slightly distorted *Z*-conformation. Therefore, even lower NOE enhancement could be expected in **3** compared to **1**.

Fortunately, we noticed the NOE enhancement in **3a** of similar magnitude to that of **1a**. Irradiation of the N-CH_3 showed 0.32% NOE enhancement for both *ortho*-protons H4/8 ($d_{H\text{-}H(XRay)}$ = 2.52 Å) that confirms its *Z*-conformation in solution. As expected (see the NOE effects for the respective **E-1c** and **1c-Na**), slightly more than twice smaller NOE effect for (*E*)-**3c** was also observed. Moreover, an additional small NOE effect was detected for *ortho*-protons H11/15 (H17/21) both in Z-3a and E-3c which is reasonable given the spatial proximity of the respective sets of protons (Fig. 4).

Fig. 4

Cross section of ROESY spectra showing the NOE enhancement of 0.32% for (*Z*)-**3a** (left) and smaller of 0.12% for (*E*)-**3c** (right) at aromatic H4/8 protons after saturation of the *N*-methyl protons. An additional weaker enhancement of H11/15 (H17/21) is also present

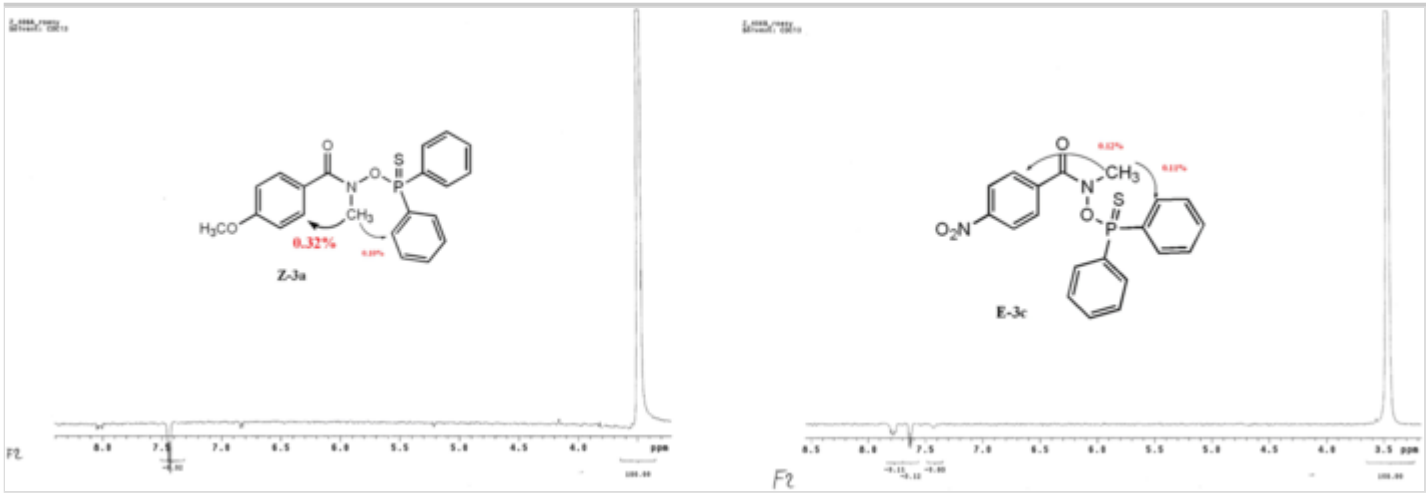

Despite the fact that NOE enhancement is also detrimental to *E* isomers, what is difficult to explain at first glance, it should be considered a convenient indicator discriminating the Z/E isomers of BHAA **1**, their salts **1-Na** and derivatives **3**.

Additional evidence confirming the preserved conformation of derivatives **3a** and **3c** is provided by the analysis of the magnitude of diamagnetic shifts of the respective protons in ^{1}H NMR spectra recorded in benzene-d_6. A larger ASIS effect (Fig. S29) was noticed for (*Z*)-**3a** (*N*-methyl signal in *Z*-**3a** is more shielded as compared to the *N*-methyl of *E*-**3c**, in accord with expectations) [40].

Previously, we found the correlation of a *para*-substituent constant on C-H proton chemical shift in *N*-isopropyl BHAA (slope 0.141 ppm) [41]. Because the analogous effect did not occur in the respective N-isopropylbenzamides, the only explanation was the existence of mixtures of Z and E isomers in different population. Thus, ^{1}H NMR spectra of N-isopropyl BHAA consist of averaged signals of both isomers while ^{1}H NMR spectra of **3** consist of only one isomer signal. *N*-Methyl proton chemical shift values are very similar ($\Delta\delta_{\mathbf{3a\text{-}3c}}$ = 0.03 ppm) that reflects their insensitivity toward *para*-substituent effect. More significant differences are noticed for the ^{13}C chemical shifts of respective *N*-methyl carbon ($\Delta\delta_{\mathbf{3a\text{-}3c}}$ = 3.8 ppm and $\Delta\delta_{\mathbf{3d\text{-}3e}}$ = 4.1 ppm) and carbonyl carbon ($\Delta\delta_{\mathbf{3a\text{-}3c}}$ = 3.7 ppm) nuclei in **3**. An increased deshielding of *N*-methyl carbon in all *Z*-isomers under the study can be correlated with at least partial pyramidalization as well as with the

lack of anisotropic effect of the carbonyl group. The high carbonyl carbon chemical shift values (173.3 ppm for *Z*-**3a**) in the range characteristic for carboxylic esters indicate also that the nitrogen pyramidalization in *Z*-**3** is preserved in solution.

NMR analysis confirmed that the aroyl residue is not affected by the arylphosphothioyl residue (similar ^{13}C chemical shifts of carbonyl carbon nuclei for **3b**, **3d** and **3e**). Also, the effect of *para*-substituent in aroyl residue on the phosphorus ^{31}P chemical shifts is not detectable ($\Delta\delta$ = 1 ppm for **3a**, **3b** and **3c**). We conclude therefore that the oxygen atom O1 bridge effectively switches off electronic transmission between the abovementioned residues.

In order to develop a more comprehensive understanding of molecular conformations of **3**, we sought to obtain infrared spectra in solution for comparison with solid-phase data (see above). In chloroformic solution, we have observed very characteristic the C=O vibration bathochromic shift ($\Delta\nu_{3aK\text{-}3aS}$ = + 10 cm^{-1}) and hypsochromic shift ($\Delta\nu_{3cK\text{-}3cS}$ = − 20 cm^{-1}) for (*Z*)-**3a** and (*E*)-**3c**, respectively (see Fig. S24 – S25). These values are far from those expected for the Z/E isomerization. Most likely, dissolution reduces or even eliminates the distortions and the strain in **3** caused by crystal packing effects, especially the lack of coplanarity between aryl and carbonyl planes and the high degree of nitrogen pyramidalization in the case of *Z*-isomers. The libration around ω_1 makes the conjugation more effective allowing para-substituents to transmit their effects toward the carbonyl group. These effects can be additionally modulated by the action of chloroform due to its known tendency to form intermolecular hydrogen bonding (C=O---$HCCl_3$). Moreover, it is worth noting that that the corresponding C=O half band widths are broader in solution which clearly indicates $\nu_{C=O}$ frequency decrease is the result of intermolecular hydrogen bonding (C=O…$HCCl_3$).

However, all abovementioned phenomena do not invert Z/E conformation for **3** acquired in the crystal state, but only modulate it, leaving it close to *Z*- or close to *E*-conformation. All presented results described above indicate that in the solution, after a dissolution of a every sample of solid **3**, its crystal structure is preserved and there is no Z/E interconversion.

Thermolysis studies

It is known that a common reaction of all hydroxylamine derivatives is a homolytic N-O bond fission due to the relative weakness of the N-O bond. Initial experiments showed that **3** undergo slow homolysis at higher temperatures. (*Z*)-**3a** and

(*E*)-**3c** stay unchanged during heating at 60 °C in C_2Cl_4 and $C_2D_2Cl_4$, respectively (Fig. S29). Upon prolonged heating at 110 °C (toluene, 10 h reflux), (*Z*)-**3a** is cleaved partially (up to 30%) to *N*-methyl-4-methoxybenzamide **5a**, exclusively (Fig. S30 and S31). Anhydrides **3** are closely related to the respective *N*-methyl *O*-thiocarbamoyl 4-X-BHAA which are known to rearrange easily at room temperature and undergo fast homolysis at 110 °C in chloroform [42]. Obviously, the reaction takes place with the participation of amidyl radicals. Therefore, compounds **3** can potentially be used in the synthesis as their source, similarly to *O*-acyl hydroxamic acids.

Heterolysis studies

It is well-known that distorted amides with a high twist angle and *N*-pyramidalization (e.g. anomeric Glover's amides [24] or 1-aza-2-adamantanones [43]) are highly reactive due to a lack of conjugation between the nitrogen lone pair and the carbonyl group [44]. As an example, DFT calculations showed that alkaline hydrolysis of a twisted formamide is exothermic, whereas the hydrolysis of the planar formamide, as well as of common amides, is highly endothermic [45].

We have found that hydrolysis and methanolysis of **3** does not occur at neutral pH at all. Also, treatment of **3** with aqueous weekly basic pyridine or trimethylamine solutions resulted only in the recovery of unchanged starting materials. It turned out that *O*-phosphothioyl benzohydroxamic acids **3** could be effectively hydrolysed in the presence of a strong non-nucleophilic base as 1,8-diazabicyclo[5.4.0]undec-7-ene (DBU). We have noticed that under these conditions **3c** and **3b** undergo much faster hydrolysis than **3a** and **3d** (the rate of hydrolysis at first glance could be correlated with Hammett parameters; Scheme 3, Fig. 5).

Scheme 3

DBU-mediated hydrolysis of 3

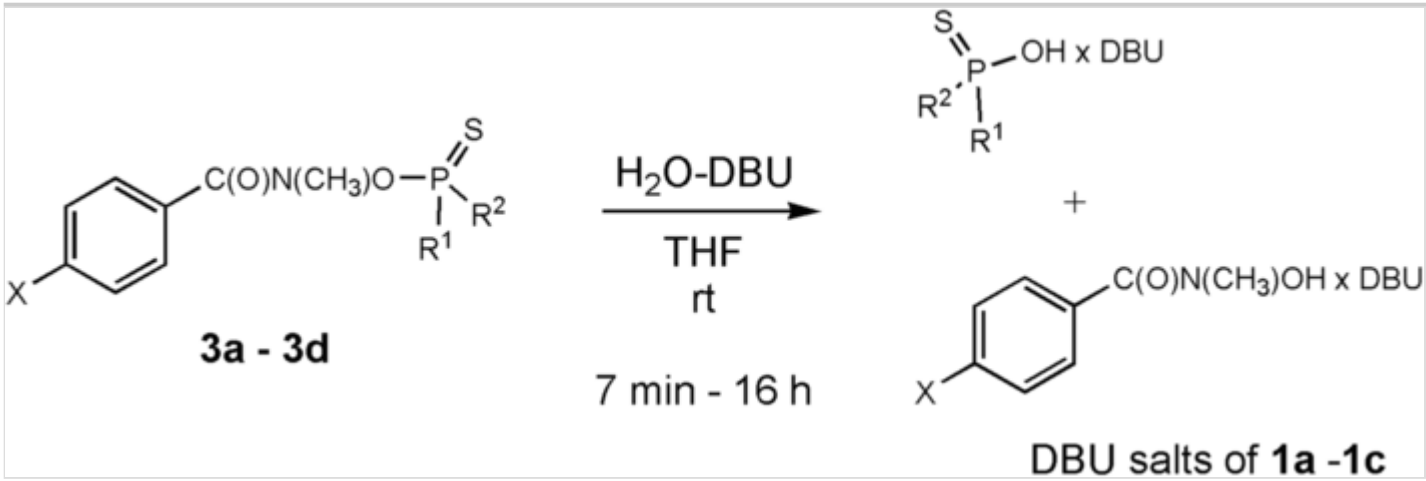

Fig. 5

Anhydrides **3a-3d** concentration decays in time during DBU-mediated hydrolysis

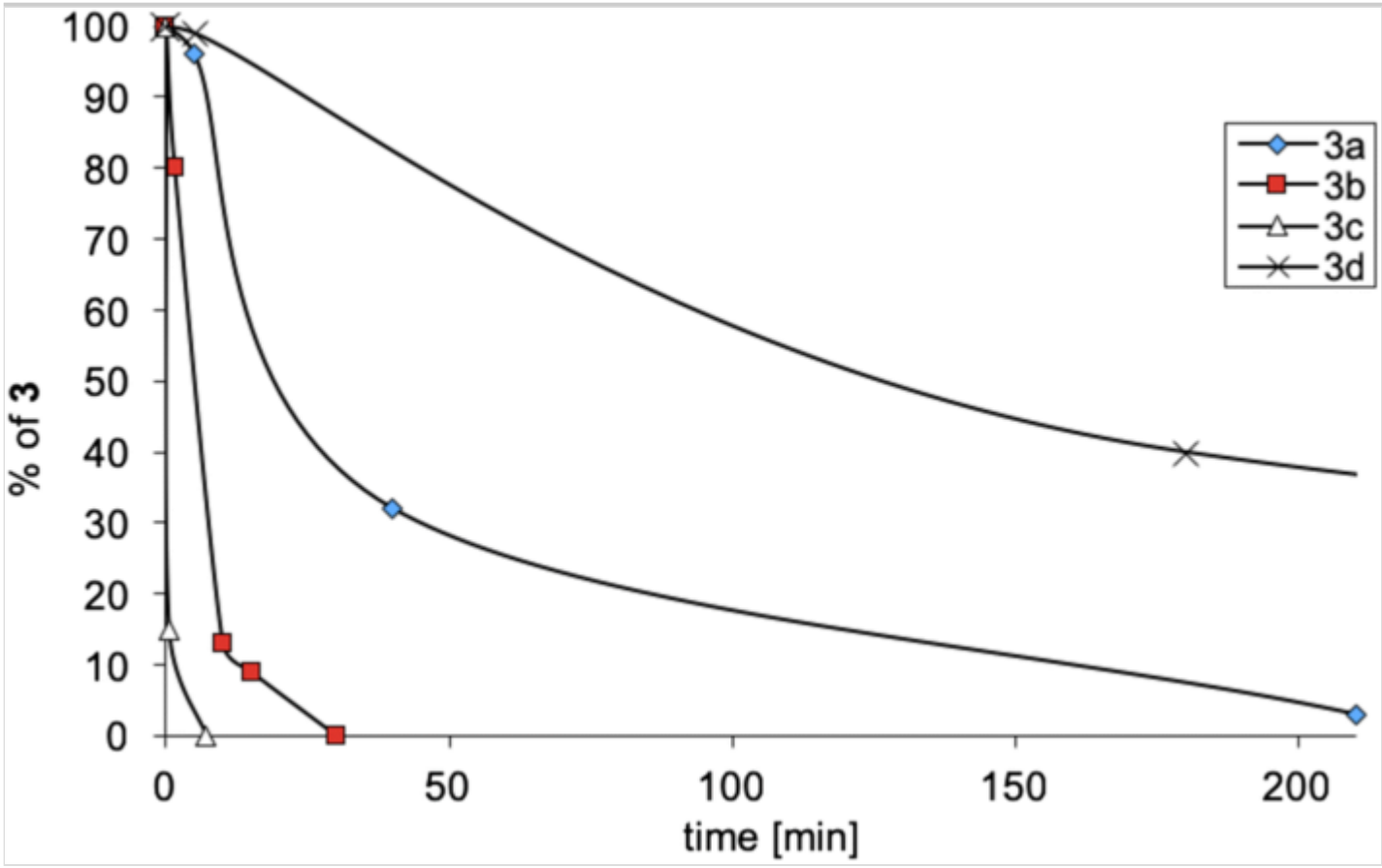

Hydrolysis of **3a** – **3c** needs two equivalents of DBU to complete (Scheme 3, Fig. S32–34), because the reaction products are relatively strong acids (hydroxamic as well as diphenylphosphinothioic acid). During their formation neutralization of DBU occurs, and their anions are too week bases to promote hydroxide anion generation. It was found that hydrolysis of **3d** requires more than three equiv. of DBU. Evidently, the enhanced inertness of **3d** is due, besides steric reasons, to the presence of the P-N bond. The N2 lone pair conjugation with the P=S bond leads to the elongation of P-S bond by 0.02 Å (see Table 2) and reduces the electron deficiency on the O-electrophilic phosphorus atom. On the other side, partial deprotonation of the acidic NH proton in the phosphonamide moiety causes a strong repulsion between the charged anion **3d**$^{-}$ and the hydroxide anion. Both processes significantly slow down the rate of hydrolysis.

Results of alkaline hydrolysis experiments using DBU confirm that hydroxide attacks phosphorus atom preferably in all cases. Additionally, all *Z*-isomers of **3** react much slower than their *E* counter isomers which seems to be contrary to expectations considering their expected higher carbonyl activity. However, because hydrolysis takes place on the electrophilic phosphorus atom not at carbonyl carbon atom, electronic effects on the phosphorus can determine reactivity of **3**. As was mentioned above, only *E*-isomers have a measurable twist angle ω_3 in solid state as well as in solution. Therefore, their enhanced reactivity is caused firstly by the presence of better leaving group (an anion of stronger hydroxamic acid) and also to a minor extent by a greater electron deficiency on the phosphorus due to a lack of coplanarity between the P=S and the P-aryl ring. In a series of **3a** – **3c**, the observed hydrolysis rate can be linearly correlated with the pKa value of conjugated hydroxamic acid (Fig. S35).

The outstanding oxyphilicity is a specific feature of anhydrides **3**. We postulate the dominant role of DBU and intermolecular assistance of the carbonyl atom in formation of transition state of the hydro- and alcoholysis reaction (Scheme 4). However, the high sensitivity of (*E*)-**3c** to hydrolysis proves that the hydrolysis rate is mainly determined by the nature of the leaving group (p-nitro benzohydroxamate $\mathbf{1c}^-$), and not by structural factors lowering the energy of the reaction transition state (for *E*-**3c**, the O2P1 bond is 0.92 Å longer and therefore weaker than in *Z*-**3a**). The established series of relativities of **3** and attempts to link their differences in susceptibility to hydrolysis with the structural factors described for the crystal state, clearly show that in solutions these compounds may assume slightly deformed Z/E conformations (see: IR spectra analysis).

Scheme 4

Proposed mechanism of heterolysis of 3 involving anchimeric assistance of carbonyl oxygen atom on the example (*Z*)-3b: DBU-mediated hydrolysis (a) and selective methanolysis in methanolic ammonia solution (b)

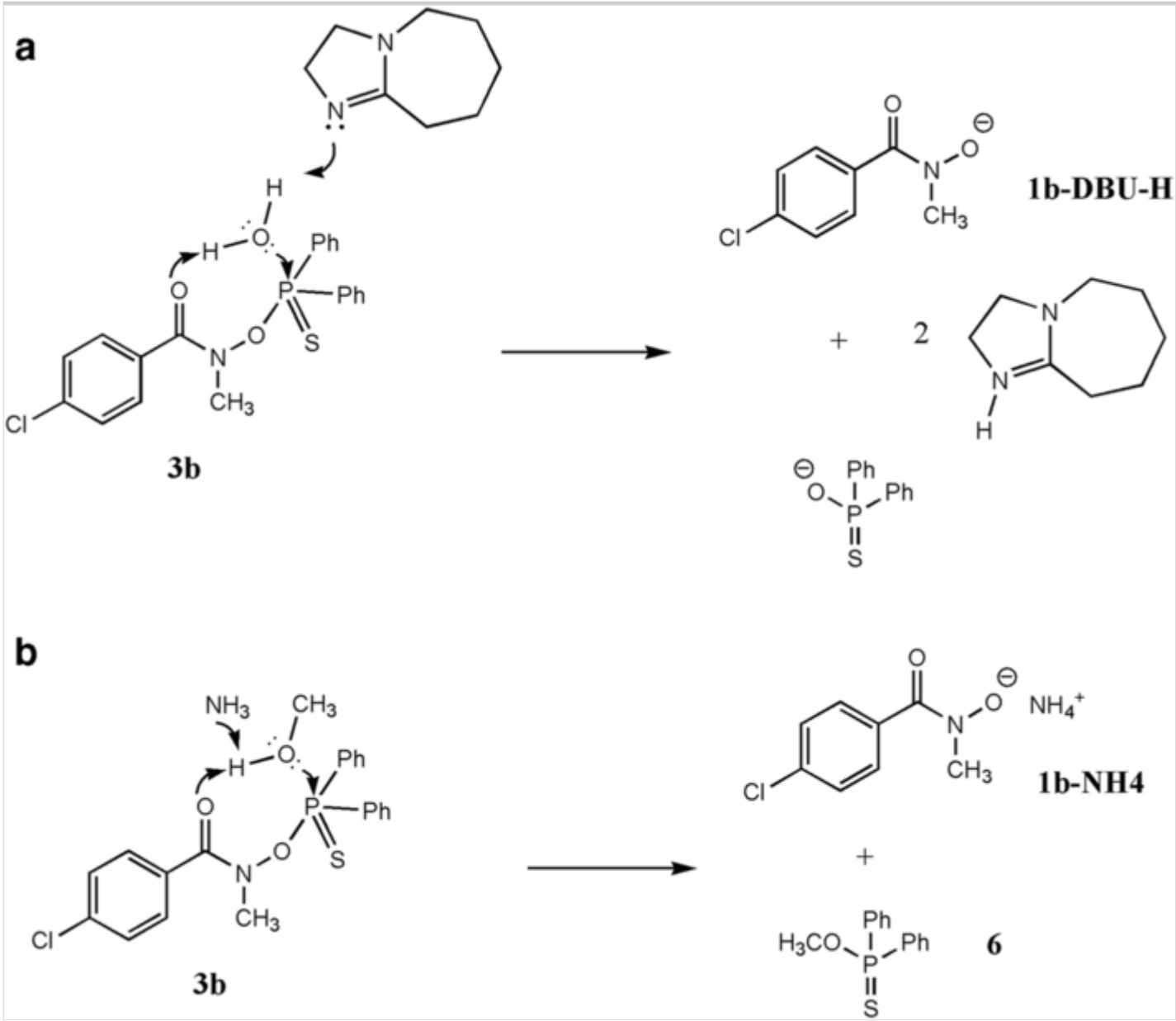

Authentic samples of diphenylphosphinothioic acid derivatives **6–8** used in heterolysis studies were obtained from chloridate **4** (Scheme 5).

Scheme 5

Reactions of phosphinothioyl chloride 4 leading to the formation of the corresponding esters 6, 7 and amide 8

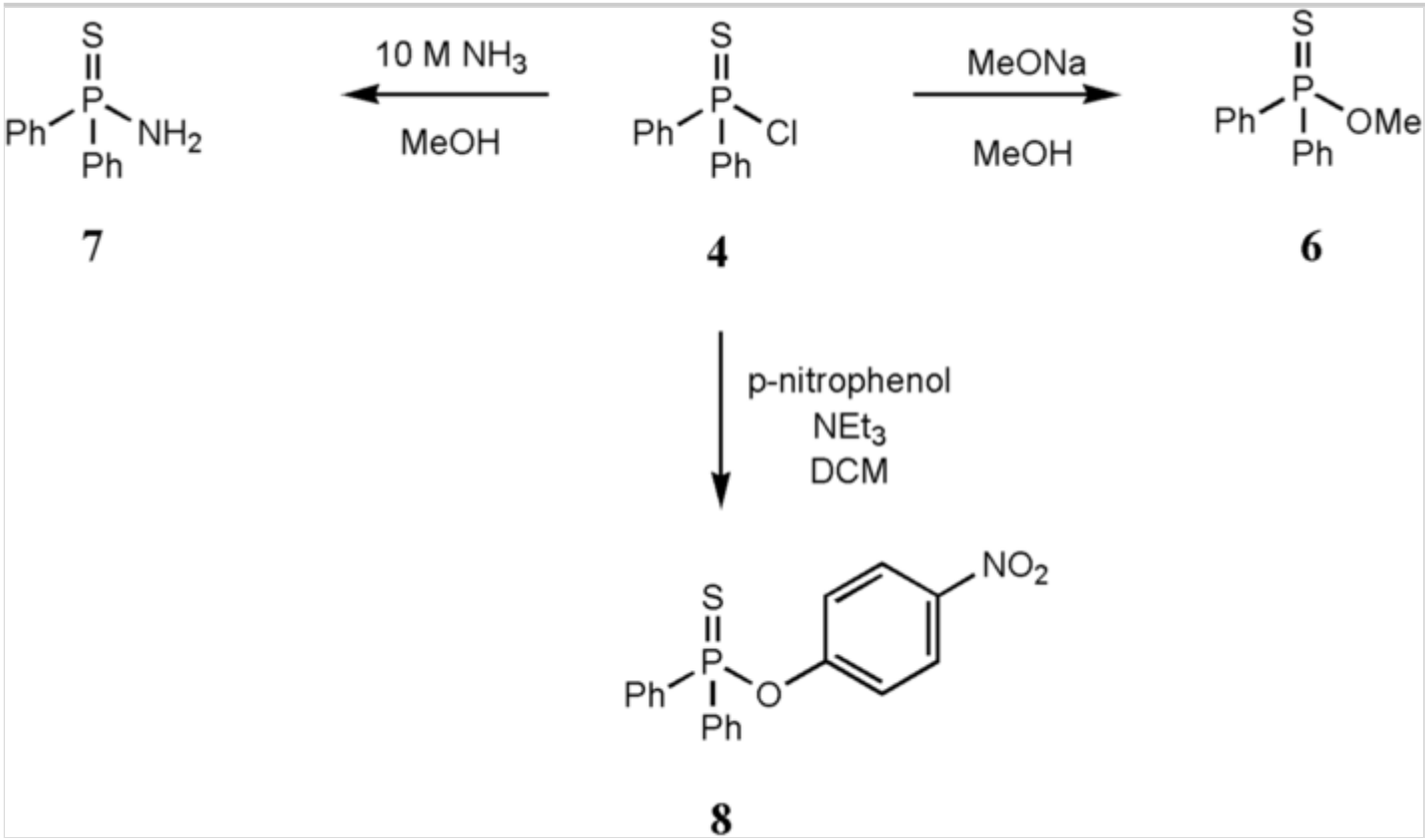

We proved that hydrolysis rate of the most reactive **3c** is comparable to hydrolysis rate of diphenyl 4-nitrophenyl phosphinothioate **8** used as a model (UV-monitored). It is not unusual since both leaving groups are the conjugate bases of acids of a comparable acidity (pKa 7.91 vs 7.15). On the other hand, we found that hydrolysis of diphenylphosphinothioyl

chloride **4** is surprisingly slower and it takes about 100 min in the same conditions (according to Harger it is complete after 2 h at 70 °C in 2 M NaOH [32]).

Ammonolysis of **3b** using saturated NH_3 methanolic solution (Scheme 4) affords unexpectedly diphenylphosphinothioic acid methyl ester $Ph_2P(S)OMe$ **6** (δ_{31P} = 85.23 ppm, Fig. S36) as the main product (93%). Therefore, chemical behaviour of **3b** is in opposite to the behaviour of $Ph_2P(S)Cl$ **4** (and also previously studied cyclic bisphosphonothioyl disulfanes or sulfanes [40]) that gives diphenylphosphinothioic acid amide $Ph_2P(S)NH_2$ **7** in the same reaction conditions, exclusively [32]. Aminolysis of **3b** using primary amine (benzylamine) as well as secondary amine (morpholine) in 1.2-M excess conducted in strictly anhydrous conditions does not proceed, leaving unchanged starting material **3b** (Fig. S37).

These results show that none of nitrogen nucleophiles attacks the electrophilic phosphorus centre in **3** probably due to a steric hindrance around phosphorus and its exceptional oxyphilicity. To our best knowledge, among phosphorus acid derivatives, only fluorides and some hindered chlorides react preferably with *O*-nucleophiles [46, 47, 48]. Therefore, hydroxide being a smaller-sized hard nucleophile/base cause quickly the P-O bond cleavage even if present in minute amounts in commercial amines, despite the known greater nucleophilicity of the later. Steric effects do not explain why ammonia is not preferred over methanol. Most probably ammonolysis is irreversible; therefore, energy gaining by forming more stable P-O bong vs P-N bond is not a reason of such chemoselectivity. We postulate a mechanism on the base of an anchimeric assistance by intramolecular general base catalysis (see Scheme 4).

On the basis of abovementioned results of experiments, we confirm that degree of N pyramidalization observed in the solid state for **3a**, **3b** and **3d** does not influence their reactivity toward O- and N-nucleophiles. According to proposed mechanism, pyramidalization is significantly diminished during the formation of the transition state with the associated nucleophile, although also some kind of relaxation should be taken into consideration upon dissolution of (*Z*)-**3**.

Conclusions and outlook

– For the five tested *O*-phosphothioyl p-substituted benzohydroxamates **3**, crystals of pure *E* and *Z* isomers can be obtained.

– Although the starting *N*-methyl benzohydroxamates exist as a mixture of both isomers in solution, the reaction mixtures always consist of one isomer of **3**. The reversibility of products **3** formation was confirmed by the performed the benzohydroxyamide group exchange reaction.

– The structure of one representative of *Z*-isomer and one representative of *E*-isomer of **3** was analysed in solution. Only one sharp signal of *N*-methyl protons in each ^{1}H NMR spectrum from − 90 °C up to 60 °C is a direct proof for conformational homogeneity of both **3**.

– NOE experiments confirmed the identity and preservation of a specific Z/E isomerism of **3**. Analysis of NMR and IR spectra showed that their conformation in solution is close to the crystal structure, and therefore is well maintained in solution.

– DFT calculations confirm the energetic preference of each specific isomer of **3** and allowed the rotation barrier to be estimated.

– The existence of only one form of **3** is not likely resulted from a different mode of its preparation but can be correlated with substituents in both the aroyl and the phosphothioyl residue influencing their stability.

– For *Z* isomers a significant nitrogen pyramidalization (38–55°; Woodward “h” parameter of 0.26–0.41 Å) does not influence their stability nor change their reactivity.

– Products **3** are thermally stable. During long-term heating above 100 °C, EDG-substituted **3** slowly decompose with the formation of the N-O bond scission products.

– A characteristic property of the compounds **3** is that they are hydrolysable but do not react with anhydrous amines as *N*-nucleophiles.

– Nucleophilic attack proceeds in every case at the phosphorus atom of products **3**, although the lack of conjugation between the nitrogen lone pair with the carbonyl group should enhance its reactivity as is the case with highly disordered amides.

– The total time hydrolysis ranges from few minutes to several days at room temperature, and the half-life of hydrolysis exhibits correlation with the pKa value of the parent benzohydroxamic acid.

– Because of their outstanding oxyphilicity, **3** can be defined as nerve agent surrogates and safer alternatives of phosphorus fluorides for AChE and other serine-active enzymes inhibition studies.

– Especially, a very wide range of their hydrolysis rates triggered by the change of substituent in the phenyl ring from nitro to methoxy group, may make them very useful as biochemical, toxicological and analytical tools.

Publisher's note

Acknowledgements

The authors are grateful to Dr. P. Sowiński for performing NMR spectra.

Authors' contributions

A.M. and W.P. carried out the experiments. J.C. performed the calculations and X-ray analyses. W.P. wrote the manuscript with support from J.C.

Funding

The studies were financially supported in part by the Polish Ministry of Science and Information Technology, grant No. 1T09A 07830.

Data availability

The authors confirm that the data supporting the findings of this study are available within the article and its supplementary materials: supplementary figures, schemes, and tables, crystallography data including ORTEP views of compounds **1b, 1c, 3a**, **3b**, **3c** and **3**d, NMR and FTIR spectra. Crystallographic data for the structures of compounds have been deposited at the CCDC as supplementary data, deposition no. CCDC No. 2010474, 2010475, 719127, 719128, 2010476, 719129 and

copies of the data can be obtained, free of charges on application to CCDC-12 Union Road, Cambridge CB2 1EZ, UK. E-mail: deposit@ccdc.cam.ac.uk.

Compliance with ethical standards

Ethical approval Ethics approval was not required for this study.

Consent to participate and consent to publish The authors have agreed for authorship, read and approved the manuscript, and given consent for participation, submission and subsequent publication of the manuscript.

Conflict of interest The authors declare that they have no conflict of interest.

Supplementary Information

ESM 1

(PDF 4946 kb)

References

1. Mukherjee S, Gupta RD (2020) Organophosphorus nerve agents: types, toxicity, and treatments. Hindawi J Toxicol:1–16. https://doi.org/10.1155/2020/3007984

2. Imrit YA, Bhakhoa H, Sergeieva T, Dan'es S, Savoo N, Elzagheid MI, Rhyman L, Andrada DM and Ramasami P (2020) A theoretical study of the hydrolysis mechanism of A-234; the suspected novichok agent in the Skripal attack. RSC Adv 10:27884–27893

3. Mian MR, Islamoglu T, Afrin U, Goswami S, Cao R, Kirlikovali KO, Hall MG, Peterson GW, Farha OK (2020) Catalytic degradation of an organophosphorus agent at Zn−OH sites in a metal−organic framework. Chem Mater

32:6998–7004

4. Gupta SP (2013) Hydroxamic acids. A unique family of chemicals with multiple biological activities. Springer-Verlag, Berlin Heidelberg

5. Miller MJ (1989) Syntheses and therapeutic potential of hydroxamic acid based siderophores and analogues. Chem Rev 89:1563–1579

6. Yet L (2018) Privileged structures in drug discovery medicinal chemistry and synthesis. Wiley, Hoboken

7. Thomas M, Alsarraf J, Araji N, Tranoy-Opalinski I, Renouxa B, Papot S (2019) The Lossen rearrangement from free hydroxamic acids. Org Biomol Chem 17:5420–5427

8. Hackley BE, Plapinger R, Stolberg M, Wagner-Jauregg T (1955) Acceleration of the hydrolysis of organic fluorophosphates and fluorophosphonates with hydroxamic acids. J Am Chem Soc 77:3651–3653

9. Sloan KB, Bodor N, Higuchi T, Little R, Wu MS (1977) Micellar acceleration of phosphorylation of hydroxamic acids: effect of chain length and of an intramolecular tertiary amino-group. J Chem Res-S:290–291

10. Shrivastava A, Ghosh KK (2008) Solvent effect on the α-effect for reaction of p-nitrophenyl diphenylphosphinate with 4-methyl 4-metoxy benzohydroxamate ion. J Mol Liq 141:99–101

11. De A, Cavalcante SF, Simas ABC, Kuca K (2019) Nerve agents' surrogates: invaluable tools for development of acetylcholinesterase reactivators. Curr Org Chem 23:1539–1559

12. Plewe MB et al (2009) Azaindole hydroxamic acids are potent HIV-1 integrase inhibitors. J Med Chem 52:7211–7219

13. Stanger KJ, Shva D, Jiang J, Krichnak V (2006) Synthesis and screening of N-alkyl hydroxamates for inhibition of cancer cell proliferation. Comb Chem High T Scr 9:651–661

14. Przychodzeń W, Nycz JE, Nam Y-J, Lee D-U (2013) Cytotoxic and antioxidant activities of benzohydroxamic acid analogues. Bull Kor Chem Soc 34:3098–3100

15. Przychodzeń W (2005) Mechanism of the reaction of Lawesson's reagent with N-alkyl hydroxamic acids. Eur J Org Chem:2002–2014

16. Przychodzeń W, Chojnacki J (2008) On the reaction of *bis*(phosphothioyl)disulfanes with hydroxamic acids I. Ionic vs radical reaction pathways. Heteroat Chem 19:271–282

17. Wuts PGM, Greene TW (2007) In: Greene's protective groups in organic synthesis4th edn. Wiley, Hoboken

18. Ikeda S, Tonegawa F, Shinozaki K, Shikano E, Ueki M (1979) Phosphinyl- and phosphinothioylamino acids and peptides. IV. Further examples of use of the diphenylphosphinothioyl group for the protection of amino acids. Bull Chem Soc Jpn 52:1431–1436

19. Hałuszczuk A, Babul N, Nierzwicki Ł, Przychodzeń W (2019) General, mild and metal-free functionalization of indole and its derivatives through direct C3-selenylation. Eur J Org Chem:4411–4416

20. Fountain KR, Fountain DP, Michaels B, Myers DB, Salmon JK, Van Galen DA, Yu P (1991) Reactivity patterns of *N*-methylbenzhydroxamates. I. Studies of methyl transfer between *N*-methylbenzhydroxamates and arenesulfonates. Can J Chem 69:798–810

21. Kabachnik MI, Mastrukova TA, Shipov AE, Melentyeva TA (1960) The application of the Hammett equation to the theory of tautomeric equilibrium. Thione-thiol equilibrium, acidity, and structure of phosphorus thio-acids. Tetrahedron 9:10–28

22. Glover SA, Rosser AA (2018) Heteroatom substitution at amide nitrogen—resonance reduction and HERON reactions of anomeric amides. Molecules 23:2834

23. Glover SA (2007) N-Acyloxy-N-alkoxyamides —structure, properties, reactivity and biological activity. Adv Phys Org Chem 42:35–123

24. Montchamp J-L (2013) Organophosphorus synthesis without phosphorus trichloride: the case for the hypophosphorous pathway. Phosphorus Sulfur Silicon 188:66–75

25. Yamasaki R, Tanatani A, Azumaya I, Masu H, Yamaguchi K, Kagechika H (2006) Solvent-dependent conformational switching of *N*-phenylhydroxamic acid and its application in crystal engineering. Cryst Growth Des 6:2007–2010

26. Przychodzeń W, Chojnacki J (2008) Conformational analysis of N-isopropylbenzohydroxamic acids: crystal structure, DFT and NMR studies. Struct Chem 19:637–644

27. Brown DA, Coogan RA, Fitzpatrick NJ, Glass WK, Abukshima DE, Shiels L, Ahlgrén M, Smolander K, Pakkanen TT, Pakkanen TA, Peräkylä M (1996) Conformational behaviour of hydroxamic acids: ab initio and structural studies. J Chem Soc Perk T 2:2673–2679

28. Kalinin VN, Yurchenko VM (1982). Zh Org Khim 48:1455–1460

29. M. J. Frisch, G. W. Trucks, H. B. Schlegel, G. E. Scuseria, M. A. Robb, J. R. Cheeseman, J. A. Montgomery, Jr., T. Vreven, K. N. Kudin, J. C. Burant, J. M. Millam, S. S. Iyengar, J. Tomasi, V. Barone, B. Mennucci, M. Cossi, G. Scalmani, N. Rega, G. A. Petersson, H. Nakatsuji, M. Hada, M. Ehara, K. Toyota, R. Fukuda, J. Hasegawa, M. Ishida, T. Nakajima, Y. Honda, O. Kitao, H. Nakai, M. Klene, X. Li, J. E. Knox, H. P. Hratchian, J. B. Cross, V. Bakken, C. Adamo, J. Jaramillo, R. Gomperts, R. E. Stratmann, O. Yazyev, A. J. Austin, R. Cammi, C. Pomelli, J. W. Ochterski, P. Y. Ayala, K. Morokuma, G. A. Voth, P. Salvador, J. J. Dannenberg, V. G. Zakrzewski, S. Dapprich, A. D. Daniels, M. C. Strain, O. Farkas, D. K. Malick, A. D. Rabuck, K. Raghavachari, J. B. Foresman, J. V. Ortiz, Q. Cui, A. G. Baboul, S.

Clifford, J. Cioslowski, B. B. Stefanov, G. Liu, A. Liashenko, P. Piskorz, I. Komaromi, R. L. Martin, D. J. Fox, T. Keith, M. A. Al-Laham, C. Y. Peng, A. Nanayakkara, M. Challacombe, P. M. W. Gill, B. Johnson, W. Chen, M. W. Wong, C. Gonzalez, and J. A. Pople, Gaussian 03, Revision D.01. Gaussian, Inc; Wallingford CT: 2004

30. Frisch MJ, Trucks GW, Schlegel HB, Scuseria GE, Robb MA, Cheeseman JR, Montgomery Jr JA, Vreven T, Kudin KN, Burant JC, Millam JM, Iyengar SS, Tomasi J, Barone V, Mennucci B, Cossi M, Scalmani G, Rega N, Petersson GA, Nakatsuji H, Hada M, Ehara M, Toyota K, Fukuda R, Hasegawa J, Ishida M, Nakajima T, Honda Y, Kitao O, Nakai H, Klene M, Li X, Knox JE, Hratchian HP, Cross JB, Bakken V, Adamo C, Jaramillo J, Gomperts R, Stratmann RE, Yazyev O, Austin AJ, Cammi R, Pomelli C, Ochterski JW, Ayala PY, Morokuma K, Voth GA, Salvador P, Dannenberg JJ, Zakrzewski VG, Dapprich S, Daniels AD, Strain MC, Farkas O, Malick DK, Rabuck AD, Raghavachari K, Foresman JB, Ortiz JV, Cui Q, Baboul AG, Clifford S, Cioslowski J, Stefanov BB, Liu G, Liashenko A, Piskorz P, Komaromi I, Martin RL, Fox DJ, Keith T, Al-Laham MA, Peng CY, Nanayakkara A, Challacombe M, Gill PMW, Johnson B, Chen W, Wong MW, Gonzalez C, and Pople JA, Gaussian, Inc., Wallingford CT, 2004

31. Harger MJP (1997) N-(Diphenylphosphinothioyl)hydroxylamine: preparation, characterisation and base-induced transposition of sulfur and oxygen atoms in its *O*-benzoyl derivative. J Chem Soc Perk T 1:3205–3209

32. Williams A, Douglas KT (1975) Aminolysis and base-catalysed hydrolysis of aryl phenylphosphonamidates and amidothionates: reactions close to the ElcB-bimolecular nucleophilic mechanistic borderline. J Chem Soc Perk T 2:1010–1016

33. Davies SG, Lee JA, Roberts PM, Thomson JE, Yin J (2011) Double asymmetric induction as a mechanistic probe: the doubly diastereoselective conjugate addition of enantiopure lithium amides to enantiopure α,β-unsaturated esters and enantiopure α,β-unsaturated hydroxamates. Tetrahedron 67:6382–6403

34. Chernega AN, Davies SG, Fletcher AM, Goodwin ChJ, Hepworth D, Prasad RS, Roberts PM, Savory ED, Smith AD, Thomson JE (2010) Alkylation and aldol reactions of acyl derivatives of N-1-(10-naphthyl)ethyl-O-tert-butylhydroxylamine: asymmetric synthesis of α-alkoxy-, α-substituted-β-alkoxy- and α,β-dialkoxyaldehydes. Tetrahedron 66:4167–4194

35. Mastryukova TA, Melentieva TA, Kabachnik MI (1965). Zh Obsh Khim 35:1197–1201

36. Brink CP, Fish LL, Crumblis AL (1985) Temperature-dependent acid dissociation constants (Ka, Δa, ΔSa) for some C-aryl hydroxamic acids: the influence of C and N substituents on hydroxamate anion solvation in aqueous solution. J Organomet Chem 50:2277–2281

37. Senthilnithy R, Gunawardhana HD, De Costa MDP, Dissanayake DP (2006) Absolute pKa determination for N-phenylbenzohydroxamic acid derivatives. J Mol Struc-THEOCHEM 761:21–26

38. Przychodzeń W, Chojnacki J (2018) Crystal structures of eight- and ten-membered cyclic bisanisylphosphonothioyl disulfanes and comparison with their P-ferrocenyl analogues. Acta Cryst E74:212–216

39. Przychodzeń W, Chojnacki J, Nierzwicki Ł (2019) Medium sized cyclic bis(anisylphosphonothioyl)disulfanes and the corresponding related cyclic sulfanes - structure and the most characteristic reactions. New J Chem 43:15413–15434

40. Lewin AH, Frucht M (1975) Restricted rotation in amides. VII - methods of resonance assignment in tertiary amides-an evaluation. Org Magn Resonance 7:206–225

41. Przychodzeń W (2006) Lawesson's reagent for direct thionation of hydroxamic acids. Substituent effects on LR reactivity. Heteroat Chem 17:676–684

42. Ankers WB, Brown C, Hudson RF, and Lawson AJ (1972) Thermal rearrangement of O-Thiocarbamoylated Hydroxamic acids: a 1,3 radical shift. J Chem Soc Chem Comm 935-936

43. Kirby AJ, Komarov IR, Feeder N (2001) Synthesis, structure and reactions of the most twisted amide. J Chem Soc Perk T 2:522–529

44. Adachi S, Kumagai N, Shibasaki M (2018) Conquering amide planarity: structural distortion and its hidden reactivity. Tetrahedron Lett 59:1147–1158

45. Lopez X, Mujika JI, Blackburn GM, Karplus M (2003) Alkaline hydrolysis of amide bonds: effect of bond twist and nitrogen pyramidalization. J Phys Chem A 107:2304–2315

46. Greenhalgh R, Weinberger MA (1967) The selective phosphylation of ethanolamine. Can J Chem 45:495–500

47. Greenhalgh R, Heggie RM, Weinberger MA (1970) Effect of the structure of phosphylating agents on their reaction with ethanolamine, an ambident nucleophile. Can J Chem 48:1351–1357

48. Hirschmann R, Yager KM, Taylor CM, Witherington J, Sprengeler PA, B. W. Phillips BW, W. Moore W, and A. B. Smith AB (1997) J Am Chem Soc 119:8177–8190